

Spectroscopy of Globular Cluster Candidates in the Sculptor Group Galaxies NGC 253 and NGC 55

M.A. Beasley & R.M. Sharples

Department of Physics, University of Durham, Durham DH1 3LE

Accepted

. Received

ABSTRACT

We have obtained spectra for 103 published globular cluster candidates in the Sculptor Group galaxies NGC 253 and NGC 55. On the basis of radial velocities and digitized plate images, 14 globular clusters are identified in NGC 253 and one probable globular cluster is identified in NGC 55. The majority of the objects in the sample appear to be background galaxies. We have obtained and analysed COSMOS plate scans of NGC 253 and NGC 55 and use these along with the spectroscopically identified clusters to define new samples of globular cluster candidates in the two galaxies which should have reduced contamination.

Key words: galaxies: individual:NGC 253 – galaxies: individual:NGC 55 – galaxies: spiral – galaxies: star clusters

1 INTRODUCTION

The search for globular clusters in external galaxies has progressed to the point where globular cluster systems have now been studied in over 100 galaxies (e.g. Harris 1999). In most cases these globular cluster systems are identified as a statistical excess of images above background, clustered around the parent galaxy. If the known globular clusters in the Galaxy are assumed to be representative of old cluster populations in external galaxies, then only in the nearest galaxies are the brightest globular clusters expected to be resolved in ground-based images (see Harris et al. 1984). The Sculptor group of galaxies forms a loose physical association of about 15 members (de Vaucouleurs 1959, 1978). At a distance of 2.5 Mpc (Graham 1982) it is generally believed to be the nearest aggregate of galaxies to our own Local Group (de Vaucouleurs 1975). Despite its relative proximity, very little is known of the globular cluster systems surrounding the major galaxies in the Sculptor group (NGC 45, 55, 247, 253, 300 and 7793). Da Costa & Graham (1982) obtained spectroscopy of three resolved cluster candidates in the field of NGC 55, an SB(s)m galaxy with $M_B = -19.7$ (de Vaucouleurs et al. 1991), and found all three to have velocities which agreed with that of NGC 55 itself. A visual search for globular cluster candidates around NGC 55 and NGC 253 has been made by Liller & Alcaïno (1983a,b) using plates from the ESO 3.6 m telescope. These authors found a total of 114 slightly diffuse objects with the $B - V$ colours, magnitudes and sizes appropriate to those of a globular cluster population similar to that in the Galaxy. A more quantitative selection of candidates was later derived by Blecha

(1986) using profile analysis of images from the Danish 1.5 m telescope.

The true nature of these globular cluster candidates, however, can only be established via spectroscopy to determine accurate radial velocities. Since these objects are marginally resolved, there is not the same level of confusion with Galactic stars as is the case with more distant cluster systems. Moreover, because the parent galaxies have low systemic velocities ($V_{N55}=129 \text{ km s}^{-1}$; $V_{N253} = 245 \text{ km s}^{-1}$) (Da Costa et al. 1991), there is little uncertainty in identifying background galaxies (see §4). In this paper we present a spectroscopic survey of the Liller & Alcaïno (1983a,b) and Blecha (1986) samples. The plan of the paper is as follows: §2 contains the observations and data reduction, with the radial velocity analysis presented in §3. In §4 we discuss the spectroscopically confirmed clusters and use this information together with COSMOS digitised plate scans to define a new sample of globular cluster candidates in §5. Conclusions are summarized in §6.

2 OBSERVATIONS AND DATA REDUCTION

2.1 Sample Selection

The sample was selected from the list of globular cluster candidates published by Liller & Alcaïno (1983a) for NGC 55, and from Liller & Alcaïno (1983b) and Blecha (1986) for NGC 253. The candidates were taken within the radial limits $0 < R < 20$ arcmin from the centres of each galaxy and magnitude limits $18 < B < 20.5$. For completeness, our candidates included twenty extra objects, six labelled 'bright' and fourteen labelled 'blue' in the Liller &

Alcaino (1983a,b) papers. Accurate astrometric positions (± 0.3 arcsec) for each target were obtained using a PDS measuring machine and reference stars from the Perth70 catalogue. At this stage any obvious galaxies (usually low surface brightness objects showing spiral structure) were expunged from the lists. The final list of candidates contained 57 objects in NGC 55 and 58 in NGC 253.

2.2 Observations

The observations were obtained with the 3.9 m Anglo-Australian Telescope (AAT) and the AUTOFIB fibre positioner (Parry & Sharples 1988) to obtain intermediate dispersion spectra of up to 64 objects within a 40 arcminute diameter field. Several fibres were used to monitor the sky background spectrum and the faint background light from the parent galaxy halo. Using a 600 lines mm^{-1} grating in first order with the RGO spectrograph, we obtained spectra covering the range 3850–5700 Å at a resolution of 4 Å using the Image Photon Counting System (IPCS) as the detector. For each galaxy 5×3000 second exposures were interspersed with 200 second exposures of a Cu–Ar–He calibration lamp and 300 second exposures of blank sky regions. Most of the observations were obtained in rather poor seeing conditions (2–3 arcsec) so the final spectra have S/N ratios typically in the range 4–20.

2.3 Data Reduction

The data have been primarily reduced using the FIGARO data reduction package with standard techniques to extract the individual spectra from the data frame and wavelength calibrate them using the exposures of the Cu–Ar–He hollow cathode lamp. The rms residuals of the wavelength calibration were typically 0.2 Å. Sky subtraction was based on the dedicated sky fibres in each frame, with the fibre-to-fibre transmission variations and vignetting along the spectrograph slit being removed using the blank sky exposures. In addition, we have corrected for the fibre-to-fibre spectral response (most of which is introduced when the spectra are extracted) using exposures of the twilight sky spectrum whose shape is assumed to be constant across the field. During the run, exposures were obtained of several bright radial velocity standards by offsetting the stars into individual fibres. The spectra consisted of 925 channels at 2 Å pixel^{-1} and prior to cross-correlation analysis were rebinned onto a logarithmic wavelength scale with a velocity step of 127 kms^{-1} per bin.

Table 1 summarizes the template objects observed for the two galaxies.

3 RADIAL VELOCITIES

Radial velocities were determined from the spectra through two methods. For obvious emission-line objects, identified lines were fitted with a gaussian and the position of the peak measured. The final velocity is the mean of these measurements for different lines, with the uncertainty being the rms between measurements. For spectra with no obvious emission lines, radial velocities were determined by the cross-correlation of object spectrum against template (Tonry & Davis 1979) with the task FXCOR in IRAF. Emission lines

Table 1. Template objects observed for NGC 55¹ and NGC 253²

Template	Object Type	Spectral Type
HD 136010 ¹	galactic star	K0 II
HD 136406 ¹	galactic star	K0 III
NGC 6356 ¹	globular cluster	G3
NGC 6809 ¹	globular cluster	F4
NGC 6981 ¹	globular cluster	F4
NGC 1851 ¹	globular cluster	F4
HD 223647 ²	galactic star	G7 III
47 Tucanae ²	globular cluster	G4
NGC 2298 ²	globular cluster	F5
HD 35410 ²	galactic star	G9 III-IV

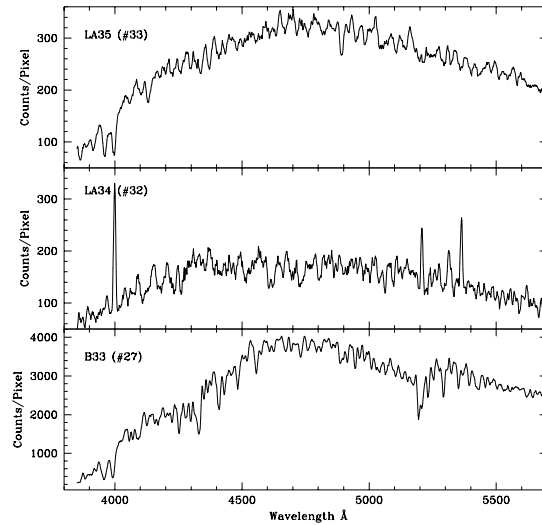


Figure 1. Spectra of globular cluster candidates around NGC 253. From top to bottom they are identified as: a globular cluster, $v_h = 228 \pm 85 \text{ kms}^{-1}$, a background galaxy, $v_h = 19830 \pm 7 \text{ kms}^{-1}$ and a foreground galactic star, $v_h = 5 \pm 7 \text{ kms}^{-1}$. The galaxy shows emission lines of [O II], [O III] and H β . The spectra have been smoothed with a 3-pixel boxcar filter.

more than 4σ from the pseudo-continuum (determined by fitting a polynomial to the spectra) where either interpolated across by hand or removed with the LINECLEAN task in IRAF. Fig. 1 shows three extracted spectra of globular cluster candidates in NGC 253.

It was required that the cross-correlations have normalised peak heights > 0.1 ; below this threshold it was found that returned velocities were unreliable and should therefore be discarded. Furthermore it was specified that each spectrum should have at least two reliable cross-correlations against different templates. The final velocities are taken to be the mean velocity weighted by the cross-correlation peak height of each template, and have been corrected to heliocentric values. The uncertainties given are the rms between velocities derived from these different templates. Tables 2 and 3 show the final velocities obtained from the candidate cluster spectra for the two galaxies. There is no real information as to the nature of external uncertainties; none of these objects have been previously observed spectroscopically and

Table 2. Globular cluster candidates in NGC 253. Columns are: ID (fibre #), heliocentric velocity, velocity error, right ascension, declination, other designation, B magnitude and classification.

ID	v_h	v_{err}	$\alpha(1950)$	$\delta(1950)$	Alternative ID ^a	B^b	Classification
1	62081	21	00 45 55.42	-25 14 19.1	LA33	18.9	galaxy
2	33731	79	00 45 17.95	-25 24 59.1	B3	20.1	galaxy
4	23061	117	00 45 19.30	-25 24 02.1	B2	21.2	galaxy
5	29601	30	00 45 19.29	-25 19 11.2	LA38	18.8	galaxy
7	212	74	00 45 35.09	-25 26 58.8	B1	21.1	cluster
8	235	28	00 45 45.79	-25 22 18.2	LA26	20.0	cluster
9	90390	12	00 46 02.22	-25 15 54.7	LAc	19.4	galaxy
10	44826	21	00 45 46.53	-25 13 02.9	LA41	19.6	galaxy
11	75687	21	00 45 00.52	-25 22 02.2	B5	20.8	galaxy
12	266	12	00 44 50.23	-25 23 24.9	LA40	19.3	cluster
13	6552	70	00 44 39.18	-25 29 28.9	B7	20.1	galaxy
14	64590	18	00 44 39.52	-25 23 43.2	B8	20.4	galaxy
17	49540	89	00 45 33.02	-25 15 14.1	LA43	19.6	galaxy
18	40825	96	00 44 58.63	-25 29 35.0	B6	21.4	galaxy
19	10230	84	00 44 44.08	-25 31 32.6	B10	21.6	galaxy
20	17940	46	00 45 54.02	-25 37 01.9	B30	19.1	galaxy
21	28484	32	00 45 58.44	-25 31 42.2	B31	19.6	galaxy
22	16857	52	00 46 11.56	-25 33 27.1	LAA	16.0	galaxy
23	72749	21	00 46 22.16	-25 32 31.8	LA12	20.0	galaxy
24	55775	117	00 45 56.23	-25 32 31.3	LA20	19.5	galaxy
25	11	10	00 46 02.64	-25 33 47.8	LA17	18.4	star
26	64353	27	00 45 38.92	-25 31 33.8	B32	20.9	galaxy
27	5	7	00 45 49.27	-25 31 00.7	B33	16.5	star
28	228	85	00 46 17.91	-25 34 48.4	LA11	20.1	cluster
29	28629	50	00 45 57.56	-25 35 47.1	LAB	16.8	galaxy
30	44961	90	00 43 51.17	-25 30 12.4	LA51	18.1	galaxy
31	41919	102	00 44 03.39	-25 25 34.5	LA52	19.2	galaxy
32	19830	7	00 43 50.18	-25 36 11.2	LA34	19.2	galaxy
33	230	14	00 43 47.77	-25 36 29.0	LA35	17.6	cluster
35	33206	167	00 43 51.01	-25 38 50.1	LA29	19.6	galaxy
36	352	26	00 44 18.06	-25 34 05.8	B15	21.0	cluster
38	70834	30	00 44 14.58	-25 20 39.9	LA56	20.0	galaxy
39	339	56	00 44 13.07	-25 20 51.9	LA57	20.3	cluster
40	401	117	00 45 05.84	-25 39 53.7	LA24	19.4	cluster
41	218	22	00 45 20.65	-25 34 03.7	B29	22.3	cluster
42	313	85	00 45 05.14	-25 37 56.2	B24	21.0	cluster
43	40796	187	00 45 52.57	-25 42 13.9	LA8	19.3	galaxy
44	447	102	00 46 04.90	-25 45 18.7	LA3	19.7	cluster
45	57852	59	00 45 45.80	-25 39 51.5	B27	19.5	galaxy
46	89151	24	00 45 20.39	-25 34 59.1	B28	21.5	galaxy
47	38485	300	00 45 24.26	-25 36 59.2	B25	21.2	galaxy
50	28236	4	00 44 44.24	-25 40 59.8	B22	21.1	galaxy
51	10233	91	00 44 38.69	-25 34 57.5	LA6	19.4	galaxy
52	20863	82	00 44 49.22	-25 32 06.3	B11	19.6	galaxy
54	22927	27	00 44 34.79	-25 40 47.3	B20	18.8	galaxy
55	9865	364	00 44 19.47	-25 40 00.8	B19	20.7	galaxy
56	39522	102	00 44 38.88	-25 34 26.6	B16	21.6	galaxy
57	361	45	00 44 55.95	-25 32 03.2	B12	20.6	cluster
58	261	52	00 44 55.64	-25 32 44.6	B13	21.4	cluster
60	21522	76	00 43 48.08	-25 38 32.7	LAC	16.1	galaxy
61	302	22	00 44 55.98	-25 33 03.1	B14	20.2	cluster
62	71064	15	00 44 34.94	-25 36 03.6	B18	21.2	galaxy
63	21020	7	00 44 32.99	-25 43 48.5	B21	20.9	galaxy
64	406	10	00 44 47.76	-25 38 49.3	B23	20.3	galaxy

^a LA \equiv Liller & Alcaino (1983b). LAB & LAc are 'blue' candidates from their sample. LAA, LAB & LAC are labelled as 'bright' objects. B \equiv Blecha (1986).^b magnitudes from Liller & Alcaino (1983b) and Blecha (1986)

Table 3. Globular cluster candidates in NGC 55. Columns are: ID (fibre #), heliocentric velocity, velocity error, right ascension, declination, other designation, B magnitude and classification.

ID	v_h	v_{err}	$\alpha(1950)$	$\delta(1950)$	Alternative ID ^a	B^b	Classification
1	66700	108	00 12 50.86	-39 17 25.9	LA61	19.0	galaxy
2	35229	101	00 12 43.09	-39 16 42.3	n	–	galaxy
3	68	4	00 12 40.60	-39 11 45.0	q	–	star
5	48	49	00 12 26.54	-39 22 12.1	k	–	star
7	32936	89	00 11 06.35	-39 39 43.8	LA5	19.8	galaxy
8	-58	80	00 12 43.35	-39 14 59.8	o	–	star
11	–	–	00 11 19.98	-39 24 55.2	LA46	19.6	QSO
12	49388	136	00 11 22.17	-39 24 23.3	LA48	19.6	galaxy
13	34933	84	00 11 05.77	-39 20 49.3	h	–	galaxy
15	26170	194	00 11 02.95	-39 16 20.8	LA58	20.7	galaxy
16	38076	123	00 11 09.12	-39 23 50.0	LA47	18.2	galaxy
17	19941	194	00 12 10.22	-39 26 17.8	g	–	galaxy
21	52918	18	00 11 08.98	-39 34 11.9	LA27	20.3	galaxy
23	96708	24	00 11 51.76	-39 32 44.5	LA36	20.6	galaxy
24	52935	24	00 11 12.27	-39 34 55.6	LA25	20.1	galaxy
25	17282	109	00 11 18.63	-39 36 06.9	LA20	19.7	galaxy
26	88804	24	00 11 13.40	-39 35 32.8	LA21	20.2	galaxy
27	-60	72	00 12 03.76	-39 29 43.2	LA45	19.8	star
29	35624	21	00 11 40.46	-39 32 56.6	LA32	18.9	galaxy
30	30855	94	00 12 28.05	-39 42 33.8	LA11	18.3	galaxy
31	26016	179	00 12 25.96	-39 42 50.8	LA9	20.5	galaxy
32	35060	14	00 12 38.50	-39 39 20.7	LA30	19.3	galaxy
33	47568	90	00 12 37.40	-39 40 28.2	LA26	19.5	galaxy
35	48265	18	00 12 09.95	-39 39 53.0	LA18	19.7	galaxy
36	71400	200	00 12 21.16	-39 42 38.3	LA8	20.2	galaxy
38	49814	108	00 12 19.71	-39 40 39.9	LA16	18.6	galaxy
39	30811	70	00 12 55.13	-39 41 44.8	t	–	galaxy
41	75000	144	00 12 57.40	-39 42 10.0	LA22	19.6	galaxy
42	74215	24	00 12 46.90	-39 44 50.0	LAd	–	galaxy
43	81546	103	00 11 55.57	-39 43 20.9	LA3	20.2	galaxy
44	32767	24	00 11 14.67	-39 40 35.8	LAb	–	galaxy
46	60311	305	00 11 54.10	-39 40 35.8	LA10	20.2	galaxy
47	30857	74	00 13 03.05	-39 43 37.4	LA15	16.9	galaxy
48	30868	62	00 13 00.49	-39 43 34.3	LA14	17.9	galaxy
49	60695	18	00 11 50.07	-39 46 19.8	a	–	galaxy
51	5089	122	00 12 52.95	-39 33 55.0	LA42	20.3	galaxy
52	52710	177	00 12 46.37	-39 35 20.7	LA39	19.2	galaxy
53	246	58	00 13 17.91	-39 35 19.7	LA43	17.1	cluster
54	37210	118	00 12 57.89	-39 36 43.5	LA37	20.4	galaxy
55	75407	27	00 12 24.29	-39 35 37.7	LA34	19.8	galaxy
56	92448	24	00 13 35.81	-39 25 23.7	LA59	20.3	galaxy
57	-142	70	00 12 28.78	-39 37 46.9	LA31	20.3	star
58	-111	23	00 13 23.85	-39 29 50.7	LA51	18.8	star
59	75971	104	00 13 29.40	-39 36 33.2	LA41	20.3	galaxy
60	31305	18	00 13 12.09	-39 37 15.9	f	–	galaxy
61	8763	39	00 11 55.37	-39 40 07.5	LAB	16.4	galaxy
62	32793	111	00 11 16.82	-39 39 21.0	LAA	16.7	galaxy
63	-29	56	00 13 02.95	-39 23 51.2	LAC	16.1	star
64	56585	12	00 12 44.39	-39 35 03.3	LA40	20.6	galaxy

^a LA \equiv Liller & Alcaino (1983a). LAb & LAd are labelled as 'blue' objects in their paper. LAA, LAB & LAC are labelled 'bright' objects. Objects here denoted n,q,k,o,h,g,t,a & f were considered by Liller & Alcaino as being too blue for classical globular clusters, but were included for completeness. B \equiv Blecha (1986).

^b magnitudes from Liller & Alcaino (1983a) and Blecha (1986)

since each field was observed solely in one setup, there are no overlaps between objects for comparison.

4 IDENTIFICATION OF GLOBULAR CLUSTERS

All our globular cluster candidates have been classified as extended objects on the basis of visual inspection of photographic plates (Liller & Alcaïno 1983a,b) or profile analysis (Blecha 1986). The main source of contamination in the samples should therefore be from background galaxies. The systemic velocity of the Sculptor group is low, ($V_{N55} = 129 \text{ km s}^{-1}$; $V_{N253} = 245 \text{ km s}^{-1}$), so we take a velocity cut at $v_h = 1000 \text{ km s}^{-1}$, with all objects above this threshold being assumed to be background galaxies. A large number of the spectra exhibited emission lines of [O II], [O III], H β or H γ and except for candidate #64 in NGC 253 (see below), these objects all had $v_h > 1000 \text{ km s}^{-1}$. Removing background galaxies in such a manner should effectively leave a sample consisting of objects which are either residual contaminating foreground Galactic stars, or globular clusters within the Sculptor group. For old clusters in the Milky Way, Armandroff (1989) gives a velocity dispersion of $\sigma = 100 \text{ km s}^{-1}$. Assuming that mass scales with σ^2 and the mass-to-light ratios of the Milky Way and the two Sculptor spirals are comparable, then the expected velocity dispersion for the halo clusters in NGC 55 and NGC 253 will be $\sim 70 \text{ km s}^{-1}$. The velocity ranges for possible clusters ($\pm 3 \sigma$ from the mean velocity) are then taken to be $-80 \leq V_{N55} \leq 340 \text{ km s}^{-1}$ and $35 \leq V_{N253} \leq 455 \text{ km s}^{-1}$ for NGC 55 and NGC 253 respectively. Since at some level there will be an overlap between high velocity foreground stars and globular clusters in the Sculptor group, distinguishing between these two cases relies on identifying true clusters as marginally extended objects.

Fifteen NGC 253 cluster candidates fall within the velocity range expected for globular clusters, and appear marginally resolved on images from the Digitized Sky Survey (see Lasker & Mclean 1994). Object #64 has $v_h = 404 \pm 10 \text{ km s}^{-1}$, but shows emission lines of [O III], H β and H γ and has therefore been excluded from further consideration. Two of the candidates, #25 and #27, have radial velocities which fall just short of the velocity cut. The appearance of their images and their COSMOS image parameters (see §5) point towards a Galactic origin; on this basis they have been identified as foreground stars. Objects #40 and #44 both have large radial velocities in comparison to the mean systemic velocity of NGC 253, with $v_h = 401 \pm 117 \text{ km s}^{-1}$ and $v_h = 447 \pm 102 \text{ km s}^{-1}$ respectively. However, the large errors reflect the significant degree of scatter between templates where the cross-correlations were close to the normalised peak height cut-off at 0.1 and so they have been left in the sample. Table 4 lists those objects in NGC 253 that are identified as globular clusters. The sample has mean velocity $\bar{v}_h = 297 \text{ km s}^{-1}$ with velocity dispersion, $\sigma = 74 \text{ km s}^{-1}$. Omitting objects #40 and #44 yields $\bar{v}_h = 276 \text{ km s}^{-1}$ and $\sigma = 55 \text{ km s}^{-1}$, this is entirely consistent with values expected for the NGC 253 globular cluster system. Twelve of the clusters fall into the 'classical' colour region for globular clusters, with $0.5 < B - V < 1.25$. Cluster #7 (B1) is very blue, with $B - V = 0.19$. Its spectrum

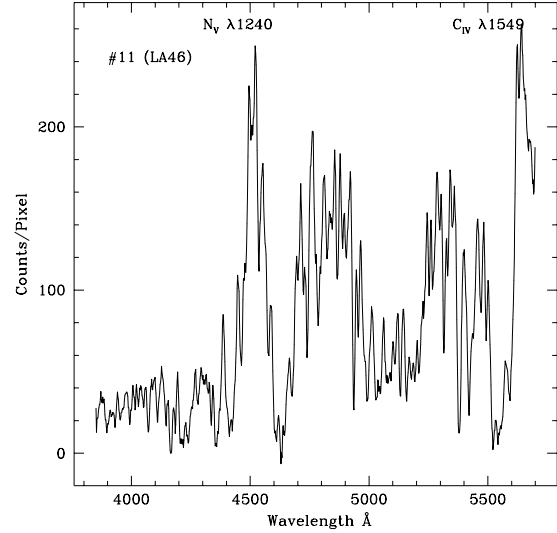


Figure 2. Object #11 in the NGC 55 cluster sample, identified as a broad absorption line (BAL) QSO at $z \sim 2.7$. Emission in N V and C IV is indicated, with their corresponding UV rest-frame wavelengths.

shows strong Balmer absorption lines, and may be analogous to the blue clusters seen in the Magellanic Clouds (e.g. Bica, Dottori, & Pastoriza 1986). Cluster #41 has $B - V = 1.8$, and is probably highly reddened due to its proximity to the disk of NGC 253 (see Blecha 1986).

In the NGC 55 sample, there are six objects that are not galaxies and fall within the velocity cut for globular clusters. However, all but one of these appear effectively point-like and lie on the stellar locus of the COSMOS plate scans (see §5). Object #53 has $v_h = 246 \pm 58 \text{ km s}^{-1}$ and lies within 2σ of the galaxies' systemic velocity. Images of this object show some elongation, but an isophotal plot indicates a round, marginally extended source blended with another object.* On the basis of this, it has been classified as a likely globular cluster. At $B = 17.1$ ($B - V = 0.76$), cluster #53 is bright but not unreasonably so. Adopting a distance modulus to NGC 55 of $(m - M)_o = 26.5$ gives the cluster $M_V = -10.2$, the same as the most luminous Galactic globular cluster ω Cen (Harris 1996).

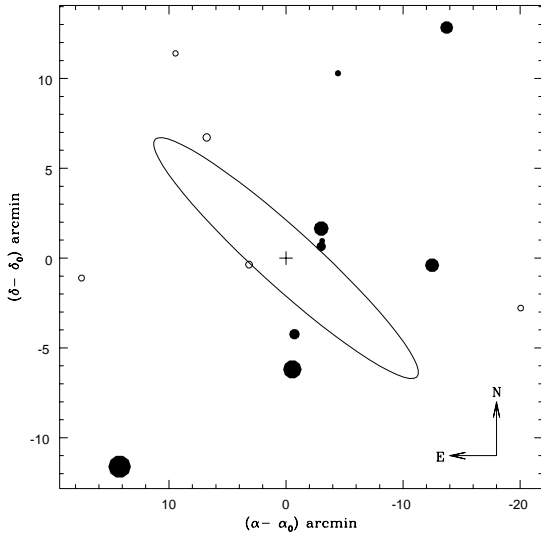
Object #11 has been identified as a broad absorption line (BAL) QSO with redshift $z \sim 2.7$. Its spectrum is shown in Fig. 2. Emission in N V and C IV is shown, though absorption shortward of N V is so strong that no Ly α emission is observed. This type of spectrum is occasionally seen in 'peculiar' BAL QSOs (e.g. Korista et al. 1995).

Fig. 3 shows the spatial distribution of the 14 objects identified as globular clusters in NGC 253. The field is approximately 40 arcminutes on a side. The distribution of cluster velocities is interesting; the clusters predominantly recede with respect to the galaxy rest-frame in the SW part of the galaxy and approach in the NE. This is consistent with the direction of rotation of the galaxy, as measured from H α rotation curves (Pence 1980). However, due to the small

* In their catalogue, Liller & Alcaïno (1983a) indicate that object #53 (LA43) is separated by $5''.9$ from a fainter companion.

Table 4. Objects in the NGC 253 sample identified as globular clusters. From left to right the columns give: ID, radial velocity, velocity error, other identification, B magnitude, $B - V$ colour and COSMOS ellipticity.

ID	v_h	v_{err}	Other ID	B	$B - V$	ϵ
7	212	74	B1	21.1	0.19	–
8	235	28	LA26	20.0	0.68	0.28
12	266	12	LA40	19.3	0.89	0.07
28	228	85	LA11	20.1	0.70	0.12
33	230	14	LA35	17.6	0.77	–
36	352	26	B15	21.0	0.94	0.23
39	339	56	LA57	20.3	0.85	0.08
40	401	117	LA24	19.4	0.97	–
41	218	22	B29	22.3	1.80	0.22
42	313	85	B24	21.0	0.86	0.22
44	447	102	LA3	19.7	0.94	–
57	361	45	B12	20.6	0.85	0.19
58	261	52	B13	21.4	0.74	0.10
61	302	22	B14	20.2	0.54	–

**Figure 3.** Distribution of globular clusters about NGC 253. Symbol size represents the magnitude of the globular cluster radial velocity with respect to the galaxy rest frame (systemic velocity $V_{N253} = 245 \text{ km s}^{-1}$). Open circles are approaching clusters, filled circles indicate receding clusters in this scheme. The centre of the coordinate system is that of NGC 253, $\alpha(1950) = 00^{\circ}45'08''$, $\delta(1950) = -25^{\circ}33'42''$. The ellipse indicates the orientation of the galaxy on the sky, with a position angle of the major axis of 50° (Pence 1980).

numbers of clusters the level of rotation is not statistically significant.

5 DEFINITION OF A NEW SAMPLE OF GLOBULAR CLUSTERS

5.1 COSMOS plate scans

The cluster samples selected by Liller & Alcaino (1983a,b) are based on visual inspection of photographic plates.

Table 5. Prime focus plates scanned using COSMOS

Plate	Object	Date	Exp. (min)	Emulsion	Filter
1739	NGC 253	20-10-79	80	IIIa-J	GG385
1740	NGC 55	20-10-79	90	IIIa-J	GG385

Clearly such selection is prone to subjective errors and saturation effects. A more quantitative approach was taken by Blecha (1986) using electronographic plates, but as can be seen from Table 2, even this sample is contaminated by both foreground stars and background galaxies. In this section we explore the use of image parameters measured by the COSMOS measuring machine (Beard, MacGillivray & Thanisch 1990) to identify new samples of globular clusters around NGC 253 and NGC 55.

AAT prime focus plates of the two Sculptor group galaxies were raster scanned with the COSMOS facility using the mapping mode, with a step size of $16 \mu\text{m}$ and a $16 \mu\text{m}$ spot size. The image area threshold was set to 10 pixels (plate scale $15.3 \text{ arcsec mm}^{-1}$), with all pixels above this threshold being grouped into discrete objects. Details of the plates are listed in Table 5.

The COSMOS image analysis software (Stobie 1982) was then run on each digitized frame to provide a list of objects with information on position, magnitude, orientation, axial ratio (major and minor axis lengths) and area. The COSMOS instrumental magnitudes were calibrated using the photoelectric sequences of Hanes & Grieve (1982), and Alcaino & Liller (1984).[†] Alcaino & Liller give V magnitudes and colours for 24 stars down to $V = 16.95$ ($B - V = 0.59$) in the field of NGC 55, and for 19 stars to $V = 16.53$ ($B - V = 0.74$) in the vicinity of NGC 253. Those from Hanes & Grieve are somewhat brighter, in the range $9 \leq V \leq 14$ for the two galaxies. There are a total of ten overlaps between their photometric sequences, with six in the NGC 253 field and four in the NGC 55 field. Both give good agreement, with a mean B magnitude offset, $\Delta_B = 0.025 \text{ mag}$, $\sigma = 0.06$ and $\Delta_B = 0.045 \text{ mag}$, $\sigma = 0.03$ for NGC 253 and NGC 55 respectively. For calibration at the faint end, the cluster candidates reached down to $B \sim 21$, and a faint star ($m_B = 21.3$) from the New Luyten Two-Tenths catalogue (NLTT) (Luyten 1980) was also used for the calibration of plate J1739.[‡] Fig. 4 shows the best-fitting calibration curve for the COSMOS instrumental magnitudes for NGC 55. A least-squares fit to the data yields an rms of 0.2 mag. The photometric calibration for NGC 253 shown in Fig. 5 shows greater scatter, with $\sigma = 0.5 \text{ mag}$. The origin of this larger

[†] It should be noted for future reference that the star designated as V on their finding chart 38 for NGC 253 is tabulated as P in the paper.

[‡] There is significant disagreement between Blecha's and Liller & Alcaino's photometry. In some instances the data differs by a full magnitude for the same object. This is seen in the COSMOS data where Blecha's candidates are systematically fainter – see Blecha (1986) for more details. For internal consistency, only Liller & Alcaino's photometry was used for the calibration of the J1739 plate.

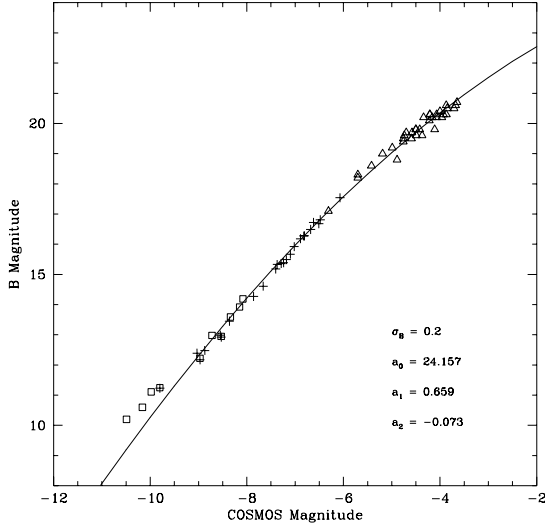


Figure 4. NGC 55: Correlation between COSMOS instrumental magnitudes and photometry of Liller & Alcaino (1983a), Alcaino & Liller (1984) and Hanes & Grieve (1982). Alcaino & Liller photometric stars are shown as crosses, Hanes & Grieve stars are open squares. Cluster candidates are shown as open triangles. A least-squares fit to the data gives a formal error in B of $\sigma = 0.2$ mag.

scatter in the NGC 253 plate is unknown, but is seen over the entire magnitude range.

An astrometric solution for the COSMOS scans was obtained so as to locate spectroscopically identified objects from this work within the COSMOS datasets. Typical astrometry plate residuals were of order ~ 0.3 arcseconds.

5.2 A New Cluster Sample

Globular clusters should appear as round, marginally extended objects on the photographic plates, whereas stars should be effectively point-like.

The ellipticity for each COSMOS object is derived from its measured image moments, where ellipticity is defined as $\epsilon = 1 - b/a$ (b and a are the measured semi-minor and semi-major axes respectively). For both plates an ellipticity limit was set at approximately three times the rms stellar ellipticity, above which threshold objects were classified as being either truly elliptical or a blend of two or more objects. These were consequently excluded from the new cluster candidate sample. Object ellipticity showed only a weak dependence on magnitude, in the sense that at fainter magnitudes the numbers of elliptical objects *marginally* increased. This was not a strong trend and fainter globular clusters should not be discriminated against in this scheme (the limits which define elliptical images increase towards fainter magnitudes.)

A powerful diagnostic to test for the extended nature of the candidates is the measured COSMOS image area as a function of magnitude. Figs. 6 and 7 show the logarithm of the image area (in pixels) against magnitude for COSMOS objects in the magnitude range $16 \leq B \leq 22$. The sharply defined sequence is the stellar locus arising from foreground stars. Extended objects show an excess of area for their mag-

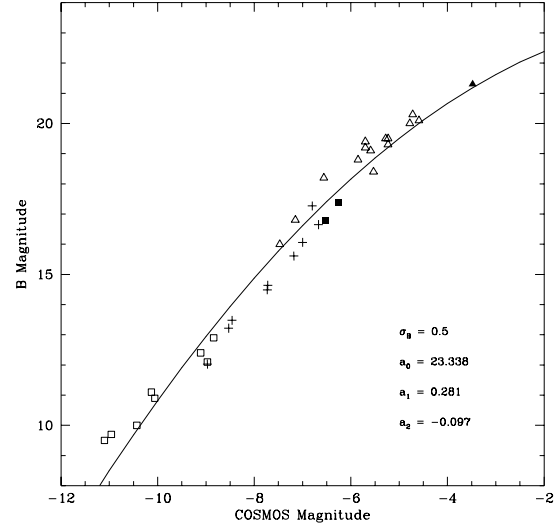


Figure 5. NGC 253: Correlation between COSMOS instrumental magnitudes and photometry of Liller & Alcaino (1983b) (open triangles), Alcaino & Liller (1984) (crosses) and Hanes & Grieve (1982) (open squares). Also plotted as a filled triangle is a faint star ($m_B = 21.3$) from the NLTT catalogue (Luyten 1980) and two additional stars from the SIMBAD database (filled squares). A least-squares fit to the data gives a formal error in B of $\sigma = 0.5$ mag.

nitude, and are raised from this sequence to some degree. Spectroscopically identified objects from this work which were located in the COSMOS data are shown. Da Costa & Graham (1982) identify three bright star clusters with $V \sim 17$ near the centre of NGC 55, one of which was returned in the COSMOS data and is indicated in Fig. 6. The two remaining clusters, along with a number of cluster candidates failed to be found. These objects are all seen in projection close to the disks of the two galaxies, and were presumably lost in the bright local background. Also, it should be noted that whilst the spectroscopic sample went out to radii comparable with that of the plate scans, NGC 253 was slightly offset from the centre of the COSMOS field, and consequently some candidates fell outside the scanning limits.

In order to quantify the excess in area shown by genuinely extended objects, and to differentiate between object types (stars, galaxies and globular clusters) a line was fit to the stellar sequence and a residual area, δA , for each object calculated. Figs. 8 and 9 show the results of this exercise, where $\delta A = 0$ corresponds to the stellar locus. Several points are evident from these figures. The scatter in δA is somewhat greater in NGC 253 than in NGC 55, with its the stellar locus being less well constrained (reflecting perhaps the larger photometry residuals – see §4). Those objects which lie on the stellar locus all have radial velocities consistent with foreground stars, and appear point-like on Sky Survey images. Galaxies are located well above the stars, and follow a similar distribution for both fields, with their residual areas increasing strongly as a function of magnitude. Identified globular clusters largely inhabit a parameter space *between* the stars and galaxies, though some overlap is apparent.

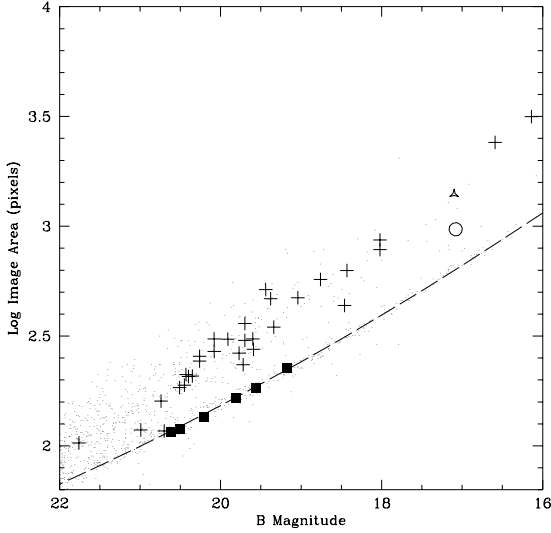


Figure 6. Log image area versus magnitude for objects in NGC 55. COSMOS objects are plotted as points, confirmed galaxies are crosses and stars are represented by filled squares. The open triangle indicates cluster #1 of Da Costa & Graham (1982) and the position of the globular cluster identified in this work is indicated by an open circle. The dashed line shows the fit applied to the stellar sequence.

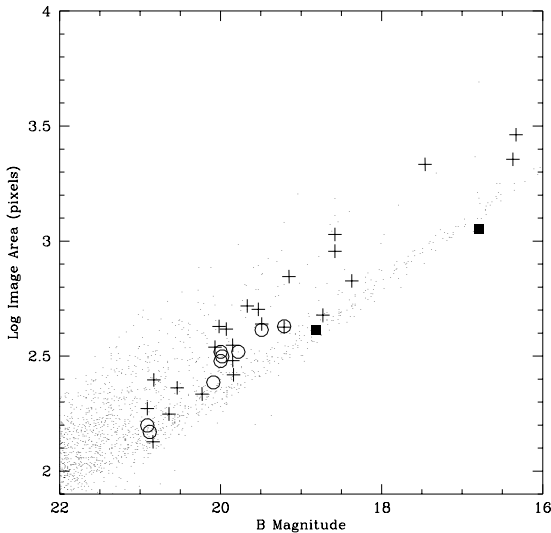


Figure 7. Log image area versus magnitude for objects in NGC 253. COSMOS objects are plotted as points, confirmed galaxies are crosses, stars are represented by filled squares and open circles indicate confirmed globular clusters.

Overplotted are the model predictions of Harris et al. (1984), scaled to the distance of the Sculptor group. These are produced by applying the COSMOS algorithm to a set of model cluster images with a range of magnitudes. The model clusters are all generated with King profiles (King 1962). Those shown in Figs. 8 and 9 have $r_t/r_c = 30$, though models with other concentration parameters ($r_t/r_c = 6 - 100$) show similar characteristics. Model clusters shown with size = 1

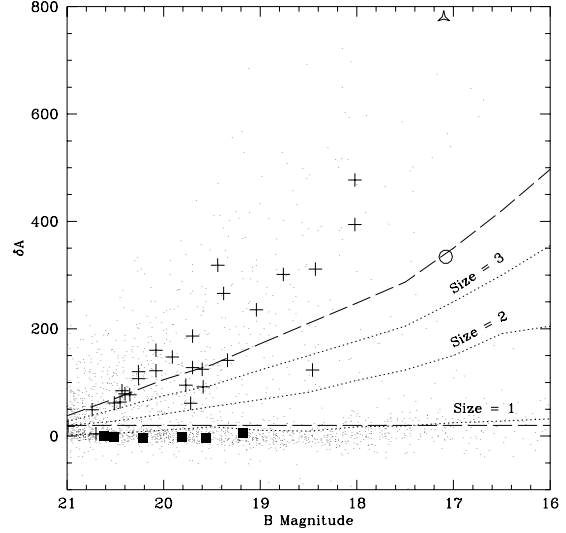


Figure 8. Area residuals of round candidates in NGC 55. The residual $\delta A = 0$ corresponds to the stellar locus. Confirmed galaxies are shown as crosses, stars are indicated by filled squares. The probable globular cluster is shown as an open circle. Dotted lines are the cluster models of Harris et al. (1984). The long dashed lines indicate the parameter space containing new globular cluster candidates.

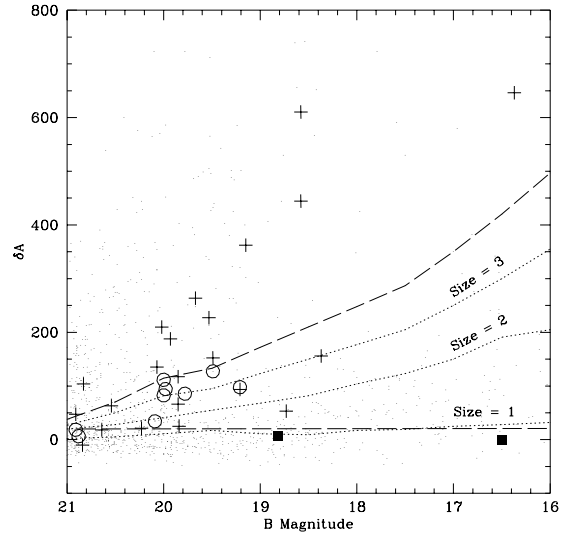


Figure 9. Residuals in area for objects in the NGC 253 field. Symbols are as for previous figure.

possess core radii of 1.5 pc and tidal radii of 45 pc (0.15 and 4.6 arcsec respectively at 2 Mpc.) Sizes 2 and 3 are correspondingly twice and three times as large. Six of the spectroscopically identified globular clusters in NGC 253 lie below the size = 3 model line, with the remaining three lying marginally above this. The apparent size of clusters on the sky will be sensitive to the assumed distance to the two galaxies, and as pointed out by Harris et al. (1984), each plate exhibits slightly different behaviour due to saturation effects and their individual isophotal thresholds (in fact they

indicate that magnitudes can be in error by as much 0.6 mag for the most extended globular cluster candidates.) The cluster of Da Costa & Graham (1982) shown in Fig. 8 shows characteristics more like that of the galaxies than the other globular clusters, though DSS images of this object show an extremely bright and crowded background which could possibly confuse the analysis software.[§]

The regions of parameter space which should contain many globular clusters are delimited in Figs. 8 and 9 by the long dashed lines. The lower limit (above the stellar locus) is set to be 3σ from the mean stellar area residual. The upper limit corresponds to approximately size = 4 model clusters and was chosen so as to include as many cluster candidates as possible, whilst minimizing contamination from background galaxies. The degree of crowding increases significantly at fainter magnitudes, therefore a magnitude cut at $m_B \leq 20.5$ has also been taken. As a final measure, images of each of the candidates have been visually examined for obvious stellar appearance or any structure indicative of a background galaxy. Some 20 objects in total were identified as being obviously 'non-cluster-like' and were removed from the sample. From the initial datasets, 91 cluster candidates have been identified in NGC 253 and 84 in NGC 55. Table 6 lists the positions and approximate B magnitudes of the new cluster candidate samples.

An idea of the contamination in the new globular cluster samples by background galaxies can be gained from a scaling of the relative numbers of spectroscopically identified objects within the defined parameter space. For the NGC 253 sample, there are 7 globular clusters and 7 background galaxies. Assuming that there are no foreground stars in the new cluster samples, then we expect to obtain ~ 45 clusters in the new NGC 253 sample. In the case of NGC 55, there are 6 galaxies and one globular cluster within the sample limits, giving an expected ~ 14 globular clusters in our sample.

The specific frequencies of the two galaxies may be calculated from an estimate of their total cluster populations. The turn over in the Galactic globular cluster luminosity function (GCLF) occurs at $M_V = -7.6$, $\sigma = 1.2$ (Harris 1999). At a distance of 2.5 Mpc for the Sculptor group, this corresponds to $B = 19.9$ ($B - V = 0.5$). Therefore the cluster candidate selection cut reaches some ~ 0.6 magnitudes past the turnover. This implies a total cluster population of approximately 60 for NGC 253, which, with $M_V = -20.0$, yields a specific frequency, $S_N = 0.6$. Applying the same arguments for NGC 55, an SB(s)m galaxy with $M_V = -19.5$ yields an expected total cluster population of approximately 20 and $S_N \sim 0.3$.

6 CONCLUSIONS

We have identified 14 globular clusters in the spiral galaxy NGC 253, and one possible globular cluster belonging to

NGC 55. Using digitized plate scans combined with spectroscopically identified stars, galaxies and globular clusters has allowed us to create new samples for the two galaxies which we expect will contain many new globular clusters.

Automated image searching techniques provide an efficient and, more importantly, quantitative way of identifying globular clusters from digitized wide-field photographic plates. Nevertheless, locating a small number of objects which can exhibit a range properties from within an initially large dataset is not straightforward, and automated searches *still* need to be supplemented by visual examination to minimize contamination from other sources. The level of contamination in the Liller & Alcaïno (1983a,b) and Blecha (1986) samples indicates the difficulty faced when undertaking searches of this type based on geometrical and/or photometric properties, especially in relatively poor cluster systems.

[§] There is little chance of a misidentification by Da Costa & Graham between their globular cluster and a background galaxy. They obtain a radial velocity for their cluster of $v_h = 106 \pm 8$ kms⁻¹ and it is seen in projection against the stellar light of NGC 55.

Table 6. New globular cluster candidates in NGC 253 and NGC 55

NGC 253				NGC 55			
ID	$\alpha(1950)$	$\delta(1950)$	B	ID	$\alpha(1950)$	$\delta(1950)$	B
1	0 44 7.68	-25 39 16.1	18.37	1	0 13 3.46	-39 38 55.7	18.69
2	0 46 44.19	-25 29 40.4	18.46	2	0 12 57.83	-39 26 3.6	18.70
3	0 46 59.32	-25 30 24.6	18.47	3	0 14 24.19	-39 15 25.7	18.72
4	0 43 54.34	-25 9 47.0	18.53	4	0 10 47.66	-39 37 41.6	18.72
5	0 44 26.32	-25 34 44.3	18.54	5	0 15 0.86	-39 35 45.1	18.86
6	0 47 1.08	-25 39 17.8	18.60	6	0 11 29.17	-39 19 43.2	18.87
7	0 46 54.30	-25 36 15.5	18.67	7	0 11 1.67	-39 53 41.0	18.87
8	0 44 8.25	-25 22 19.4	18.68	8	0 13 48.19	-39 14 29.4	18.91
9	0 44 47.79	-25 32 9.6	18.76	9	0 12 42.25	-39 1 49.5	18.93
10	0 46 13.33	-25 28 37.7	18.80	10	0 11 42.33	-39 25 8.1	19.03
11	0 45 17.67	-25 9 38.2	18.83	11	0 12 8.84	-39 25 59.1	19.08
12	0 46 33.06	-25 40 55.7	18.83	12	0 12 0.20	-39 28 45.6	19.12
13	0 43 45.23	-25 23 9.1	18.90	13	0 14 4.81	-39 23 47.1	19.14
14	0 43 47.97	-25 17 58.8	18.98	14	0 12 52.24	-39 42 50.1	19.14
15	0 46 37.88	-25 28 42.6	18.99	15	0 12 15.83	-39 44 26.2	19.14
16	0 44 42.51	-25 39 44.7	19.00	16	0 14 25.55	-39 33 18.0	19.17
17	0 44 39.09	-25 18 22.5	19.02	17	0 12 45.44	-39 44 12.0	19.17
18	0 45 29.49	-25 21 44.1	19.14	18	0 12 47.47	-39 10 42.2	19.19
19	0 46 39.13	-25 22 34.6	19.20	19	0 13 7.21	-39 57 19.7	19.19
20	0 46 29.39	-25 34 10.0	19.21	20	0 14 49.86	-39 20 0.3	19.22
21	0 44 47.55	-25 39 16.4	19.23	21	0 14 49.49	-39 35 7.6	19.22
22	0 46 52.64	-25 23 35.8	19.25	22	0 12 55.67	-39 46 29.9	19.26
23	0 43 54.16	-25 30 53.1	19.27	23	0 13 4.33	-39 43 43.7	19.30
24	0 43 40.58	-25 14 40.3	19.33	24	0 12 42.38	-39 6 13.5	19.32
25	0 43 43.70	-25 19 50.2	19.41	25	0 14 41.43	-39 35 14.1	19.33
26	0 44 2.69	-25 11 29.1	19.42	26	0 14 40.96	-39 23 13.0	19.34
27	0 44 24.04	-25 19 48.0	19.43	27	0 14 7.81	-39 14 38.9	19.37
28	0 45 8.48	-25 34 55.7	19.43	28	0 13 1.59	-39 52 22.8	19.40
29	0 44 47.84	-25 29 55.3	19.46	29	0 14 6.12	-39 28 15.2	19.42
30	0 46 18.62	-25 12 10.8	19.54	30	0 10 35.36	-39 19 12.2	19.44
31	0 46 7.82	-25 31 25.5	19.54	31	0 11 30.20	-39 24 56.6	19.44
32	0 45 20.82	-25 35 0.5	19.56	32	0 11 45.84	-39 27 33.7	19.49
33	0 44 36.24	-25 13 3.8	19.58	33	0 13 1.89	-39 31 30.6	19.51
34	0 46 27.09	-25 17 27.8	19.62	34	0 13 28.69	-39 40 53.4	19.52
35	0 43 56.76	-25 26 6.5	19.73	35	0 13 12.97	-39 48 35.3	19.52
36	0 46 20.53	-25 7 30.0	19.74	36	0 13 37.10	-39 41 1.9	19.53
37	0 44 26.05	-25 33 27.7	19.78	37	0 12 1.03	-39 38 13.4	19.56
38	0 44 23.19	-25 34 27.1	19.78	38	0 13 10.13	-39 29 22.5	19.59
39	0 45 5.08	-25 41 4.9	19.78	39	0 12 37.46	-39 40 27.5	19.59
40	0 45 26.88	-25 14 3.7	19.80	40	0 12 56.36	-39 11 5.5	19.61
41	0 46 38.15	-25 38 5.1	19.84	41	0 12 24.07	-39 21 38.4	19.66
42	0 45 17.95	-25 7 18.2	19.85	42	0 13 16.92	-39 30 21.8	19.69
43	0 44 21.09	-25 9 56.4	19.85	43	0 11 15.90	-39 41 46.8	19.72
44	0 44 13.97	-25 16 45.2	19.89	44	0 13 27.56	-39 31 8.2	19.74
45	0 46 11.34	-25 34 21.7	19.89	45	0 13 48.31	-39 32 42.0	19.77
46	0 43 36.63	-25 25 59.0	19.92	46	0 11 44.80	-39 52 46.7	19.77
47	0 45 37.20	-25 30 0.9	19.92	47	0 13 43.24	-39 16 23.9	19.82
48	0 45 31.88	-25 13 15.9	19.93	48	0 13 7.18	-39 30 30.2	19.82
49	0 46 22.68	-25 41 22.3	19.95	49	0 12 55.83	-39 54 42.5	19.86
50	0 44 36.63	-25 35 13.0	19.96	50	0 11 54.33	-39 6 26.1	19.87
51	0 45 36.56	-25 25 22.5	19.97	51	0 14 43.92	-39 30 53.4	19.90
52	0 43 2.99	-25 29 3.3	19.97	52	0 12 23.58	-39 26 38.9	19.95
53	0 46 20.52	-25 18 24.7	19.99	53	0 12 3.73	-39 42 27.3	19.98
54	0 45 32.61	-25 19 12.7	20.00	54	0 10 41.10	-39 15 33.7	19.99
55	0 45 7.70	-25 7 49.0	20.02	55	0 10 13.53	-39 21 36.1	19.99
56	0 46 30.20	-25 18 57.3	20.02	56	0 12 3.47	-39 46 56.0	20.04
57	0 43 40.49	-25 18 60.0	20.03	57	0 11 6.42	-39 36 20.8	20.09
58	0 44 12.65	-25 25 0.7	20.03	58	0 14 21.57	-39 39 0.1	20.14
59	0 45 50.94	-25 26 24.1	20.03	59	0 14 3.89	-39 40 26.1	20.14
60	0 45 20.69	-25 24 50.2	20.04	60	0 12 46.07	-39 46 11.6	20.16
61	0 45 32.76	-25 26 14.9	20.04	61	0 13 28.03	-39 34 34.8	20.17
62	0 45 3.07	-25 26 6.2	20.05	62	0 11 30.88	-39 6 5.7	20.20
63	0 44 36.71	-25 28 30.0	20.05	63	0 13 13.77	-39 54 20.3	20.20

Table 6 – *continued*

NGC 253				NGC 55			
ID	$\alpha(1950)$	$\delta(1950)$	B	ID	$\alpha(1950)$	$\delta(1950)$	B
64	0 43 14.65	-25 21 54.9	20.09	64	0 11 36.53	-39 45 59.4	20.21
65	0 45 4.34	-25 23 34.2	20.13	65	0 11 57.43	-39 28 54.7	20.22
66	0 45 37.23	-25 23 39.7	20.17	66	0 11 23.35	-39 55 17.1	20.23
67	0 44 40.80	-25 11 6.0	20.19	67	0 11 16.33	-39 20 21.0	20.25
68	0 45 37.02	-25 25 54.8	20.20	68	0 12 36.07	-39 31 8.1	20.25
69	0 44 32.62	-25 36 32.1	20.21	69	0 13 35.26	-39 16 50.7	20.26
70	0 45 34.90	-25 12 47.7	20.25	70	0 12 58.36	-39 6 24.0	20.27
71	0 44 55.68	-25 27 17.0	20.25	71	0 12 45.49	-39 32 5.2	20.27
72	0 44 4.62	-25 33 56.6	20.26	72	0 13 43.07	-39 0 34.6	20.30
73	0 46 32.61	-25 24 17.2	20.27	73	0 12 44.11	-39 5 14.9	20.35
74	0 44 41.69	-25 41 10.1	20.27	74	0 13 47.95	-39 21 47.3	20.37
75	0 47 2.19	-25 16 21.5	20.29	75	0 12 2.75	-39 29 46.9	20.38
76	0 45 24.03	-25 27 38.9	20.30	76	0 12 47.66	-39 32 1.9	20.40
77	0 45 33.33	-25 19 35.5	20.31	77	0 13 26.69	-39 51 25.4	20.40
78	0 46 56.06	-25 15 35.7	20.32	78	0 14 20.98	-39 39 19.8	20.43
79	0 46 19.62	-25 16 33.5	20.34	79	0 13 3.11	-39 23 17.3	20.45
80	0 46 14.77	-25 26 23.3	20.34	80	0 14 54.78	-39 38 33.2	20.46
81	0 46 25.46	-25 29 25.5	20.36	81	0 13 53.54	-39 14 38.0	20.48
82	0 46 20.15	-25 17 50.8	20.38	82	0 13 39.53	-39 35 53.9	20.48
83	0 44 28.43	-25 28 57.1	20.38	83	0 13 49.87	-39 10 44.9	20.49
84	0 43 22.61	-25 21 44.0	20.40	84	0 13 25.27	-39 52 10.6	20.49
85	0 44 36.96	-25 13 5.7	20.41				
86	0 44 31.90	-25 41 39.1	20.41				
87	0 44 25.59	-25 41 47.8	20.47				
88	0 44 50.77	-25 8 33.0	20.49				
89	0 43 29.80	-25 17 5.3	20.49				
90	0 45 45.57	-25 13 2.6	20.50				
91	0 45 1.99	-25 23 58.9	20.50				

REFERENCES

- Alcaino G., Liller W., 1984, ApJ, 89, 6
 Armandroff T.E., 1989, AJ, 97, 375
 Beard S.M., MacGillivray H.T., Thanisch P.F., 1990, MNRAS, 247, 311
 Blecha A, A&A, 1986, 154, 32
 Bica E., Dottori H., Pastoriza M., 1986, A&A, 156, 261
 Da Costa G.S., Graham J.A., 1982, ApJ, 261, 70
 Da Costa L.N., Pellegrini P.S., Davis M., Meiksin A., Sargent W.L.W., Tonry J.L., 1991, ApJS, 75, 935
 Delhaye J., 1965, in Blaauw A., Schmidt M., eds, Galactic Structure, University of Chicago Press, Chicago, P.61
 de Vaucouleurs G., 1959, AJ, 130, 718
 de Vaucouleurs G., 1978, AJ, 224, 710
 de Vaucouleurs G., 1975, in Sandage A., Sandage M. and Kristian J., eds, Stars and Stellar Systems, Vol 9, Galaxies and the Universe, University of Chicago Press, Chicago, p.557
 de Vaucouleurs G., de Vaucouleurs A., Corwin J.R., Buta R.J., Paturel G., Fouque P., 1991, Third Reference Catalogue of Bright Galaxies, version 9, Springer-Verlag, New York
 Graham J.A., 1982, ApJ, 252, 474
 Hanes D.A., Grieve G.R., 1982, MNRAS, 198, 193
 Harris W.E., 1996, AJ, 112, 1487
 Harris W.E., 1999, Saas-Fee Advanced Course on Star Clusters, Swiss Society for Astrophysics and Astronomy, Springer, in press
 Harris H.C., Harris G. L. H., Hesser J.E., MacGillivray H.T., 1984, ApJ, 287, 185
 King I, 1962, AJ, 67, 471
 Korista K.T. et al., 1995, ApJS, 97, 285
 Lasker B.M., McLean B.J. 1994, ST Sci Newsletter, 11, No. 2, 39
 Liller W., Alcaino G., 1983, ApJ, 264, 53
 Liller W., Alcaino G., 1983, ApJ, 265, 166
 Luyten W.J., 1980, NLTT Catalogue, University of Minnesota
 Parry I., Sharples R.M., 1988, in Barden S.C., ed, ASP Conference Series, Volume 3, Fibre Optics in Astronomy, San Francisco, ASP, p.93
 Pence W.D., 1980, ApJ, 239, 54
 Stobie R.S., 1982, COSMOS User Manual (Royal Observatory Edinburgh)
 Tonry J., Davis M., 1979, AJ, 84, 10